Progress In Electromagnetics Research C, Vol. 104, 215–228, 2020

Sub-Domain Analysis of Asymmetrical Magnetic Field in Electrical Machines

Sohrab Amini Velashani and Jawad Faiz*

Abstract—Beside magnetic equivalent circuit and finite element methods, sub-domain analysis (SDA) is an alternative method, which can be used to evaluate electrical machines behavior. It has a reasonable accuracy, and its parametric nature is allowed to apply to optimization or sensitivity analysis. Commonly, this method is based on variables separation technique of Maxwell equations and Fourier series. Eigenvalues and eigen-functions are so important for obtaining accurate results. In this paper, Maxwell equations are solved for two adjacent regions, i.e., copper (Cu) and permanent magnet (PM). It was paid less attention before, and it introduces supplementary eigenvalue and eigen-function for asymmetry conditions in Cu or PM magnetic field regions.

1. INTRODUCTION

There are different methods for electrical machines analysis, and applications of these methods depend on the required accuracy and results [1–3]. Magnetic equivalent circuit is normally employed for quick analysis with acceptable but low accuracy. The method offers the equivalent components of machine elements, and magnetic field is then estimated based on the mean value of the magnetic flux in every cross-section. Electrical equivalent circuits and state equations are applicable to precise analysis. In this case, circuit elements are determined based on estimations which are more precise based on measurement or calculations; meanwhile, transient operation can also be analyzed. Numerical analyses, such as finite element method (FEM), are utilized for more accurate and detailed solution, but these techniques are time consuming and involve long computation time to establish a model. In addition, it needs an appropriate processor for two-dimensional (2D) or three-dimensional (3D) analysis of steady-state and transient modes. Meantime, there are boarder lines methods such as layer analysis technique, which are mostly used in linear electrical machines.

Generally, sub-domain analysis (SDA) not only has enough accuracy but also does not involve application of powerful processors, and its computation time is shorter than numerical methods. In the SDA, the geometry of electrical machine is divided into defined domains taking into account its application and existing symmetries [4]. Maxwell equations, here Laplacian and Poisson equations, are written for every region, and finally based on the imposed boundary conditions on the regions, such as continuity of magnetic potential and magnetic field intensity tangential component, the required system of equations for magnetic field is formed and then solved [5, 6]. Generally, variables separation technique (VST) has a very significant role; however, in some electromagnetic problems it is necessary to establish the equations for solving Laplacian and Poisson equations [7]. Some have reported the application of SDA for different electrical machines such as surface-inset PM [6–8], surface-mounted PM [9], interior PM [10, 11], PMSM with shielding cylinder [12] spoke type PM [2], doubly-salient machine [13], switched reluctance machine [14, 15], Vernier machine [5, 16], flux switching machine [17], superconductor [18], and electric machine with toroidal winding [19]. Normally, the results have been

Received 18 June 2020, Accepted 4 August 2020, Scheduled 17 August 2020
* Corresponding author: Jawad Faiz (jfaiz@ut.ac.ir).
The authors are with the Centre of Excellence on Applied Electromagnetic Systems, School of Electrical and Computer Engineering, College of Engineering, University of Tehran, Tehran 1439957131, Iran.

compared with FEM results and in some cases tests results. In addition, some have considered the iron parts in SDA [2, 3]. Generally, based on the above-mentioned works, this method considers the chosen eigen-function and assumes that the horizontal and vertical components of magnetic field in PMs and slots are merely odd and even functions, respectively. In addition, they assume that these components in conductors are even and odd functions (dual of PM magnetic fields). In fact, deviation of the magnetic field due to the presence of redundant components in PM and slot and/or Cu is neglected; therefore, it may accrue major errors in magnetic fields of PMs/slots or Cu. Besides, it assumes that PM or Cu conductor is generally adjacent the ideal iron or air gap, and then field equations are established based on this configuration, while in some electric machine configurations, the PMs may be placed near the Cu, and thus, it is important to extract field equations for this situation. Therefore, in this paper the above-mentioned assumptions are addressed, and the field equations in PM and Cu are extracted more precisely. In addition, the system of equations for two regions of the PM and adjacent Cu is determined and verified.

2. PM REGION

Based on Figure 1 and assuming a constant magnetic momentum, the governing equation of the PM part is as follows [20]:

$$\overrightarrow{M} = M\hat{j} \tag{1}$$

$$\frac{\partial^2 A_{pm}}{\partial^2 x} + \frac{\partial^2 A_{pm}}{\partial^2 y} = 0 \tag{2}$$

In addition, there are the following governing equations on the PM boundaries:

$$\hat{n} \times \left(\overrightarrow{H_{tm}} - \overrightarrow{H_{ti}}\right) = J\hat{k} \tag{3}$$

$$J = M \tag{4}$$

$$H_{ti} = 0 \tag{5}$$

$$H_{tm}|_{x=\frac{w}{2}} = -\frac{1}{\mu_0}\frac{\partial A_{pm}}{\partial x} = -M \tag{6}$$

$$H_{tm}|_{x=-\frac{w}{2}} = -\frac{1}{\mu_0}\frac{\partial A_{pm}}{\partial x} = -M \tag{7}$$

The above equations are Laplacian equation with non-homogenous boundary conditions. To use the VST, it is necessary to convert it to homogenous equation with homogenous boundary conditions. At this end, based on the superposition principle, the following function is defined to convert the main equations as homogenous one:

$$A_{pm}(x, y) = U(x, y) + V(x, y) \tag{8}$$

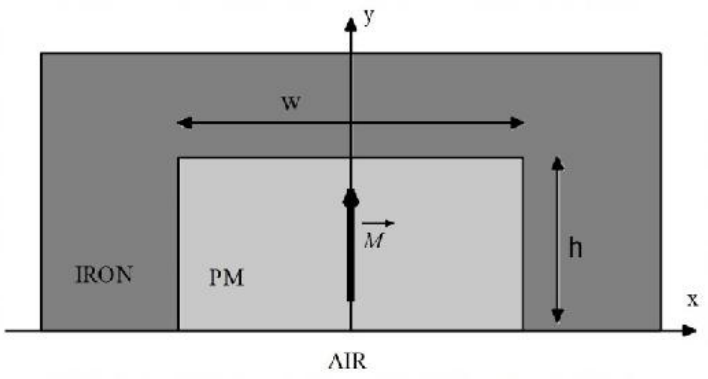

Figure 1. PM region.

$$\frac{1}{\mu_0}\frac{\partial V}{\partial x} = M \tag{9}$$

Therefore,

$$V(x,y) = V(x) = \mu_0 M x + k_1 \tag{10}$$

Considering the problem form and boundary conditions, the equivalent homogenous response can be written as follows:

$$U(x,y) = \sum_n \cosh[k_n (y-h)][a_n \sin(k_n x) + b_n \cos(k_n x)] \tag{11}$$

Substituting Eqs. (10) and (11) into Eq. (2), only the Laplacian of U will remain, which after derivation will also vanish. Boundary conditions are also satisfied by replacing Eq. (8) in Eqs. (6) and (7).

By applying the boundary condition $x = \pm 0.5w$, we have:

$$\begin{aligned} k_n \left[a_n \cos\left(k_n \frac{w}{2}\right) + b_n \sin\left(k_n \frac{w}{2}\right)\right] = 0 \\ k_n \left[a_n \cos\left(k_n \frac{w}{2}\right) - b_n \sin\left(k_n \frac{w}{2}\right)\right] = 0 \end{aligned} \tag{12}$$

Therefore,

$$\begin{aligned} a_n \cos\left(k_n \frac{w}{2}\right) = 0 \\ b_n \sin\left(k_n \frac{w}{2}\right) = 0 \end{aligned} \tag{13}$$

Since k_n in Eq. (12) cannot be determined as such that both equations become correct without having non-zero coefficients, it is necessary, at least in one of the equations, the equivalent coefficient tends to zero. Considering that the vertical component of the magnetic flux density of the PM in Figure 1 is even function with respect to the PM axis, and its horizontal component is odd, it can be expected that the first equation has non-zero coefficient, in other words:

$$\begin{aligned} a_n \neq 0 \\ b_n = 0 \end{aligned} \tag{14}$$

Therefore, based on Eqs. (13) and (14), the eigenvalues and eigen-functions are obtained as follows:

$$k_n = \frac{(2n-1)\pi}{w}, \quad n = 1, 2, 3, ... \tag{15}$$

$$f_n(x) = \sin\left(\frac{(2n-1)\pi}{w} x\right) \tag{16}$$

Finally,

$$A_{pm}(x,y) = \mu_0 M x + k_1 + \sum_n a_n \cosh\left[\frac{(2n-1)\pi}{w}(y-h)\right] \sin\left(\frac{(2n-1)\pi}{w} x\right) \tag{17}$$

As shown in Figure 1, if the geometry of the machine is symmetrical with respect to the PM axis in the PMs established region, Eq. (17) coincides with this geometry, and it is predicted that Eq. (17) well models the magnetic behavior of the PM region (Figure 2(a)). When we push the geometry to asymmetrical position such as Figure 2(b), the magnetic flux lines alter as such that they are placed in paths with minimum reluctance, and therefore, there may be no any symmetry in magnetic fields in regions such as PM. For example, Figure 3 shows the vertical component of magnetic flux density on a hypothesis line. As seen, when the geometry is asymmetrical, the magnetic flux density is not even function, and therefore, it is not possible to model this component with merely one eigen-function (cosine function derived from Eq. (17)). This situation goes worse when we insert a current component into the model. Because the magnetic fields usually turn the Cu conductors, the magnetic flux lines due to the Cu fields may enter the PMs and vice versa, and finally, it leads to more asymmetry in PM or Cu magnetic fields. In Figure 2(c), Cu has been replaced with air slot, and as seen the magnetic flux lines have been changed significantly based on the magnetic flux contours caused by Cu current.

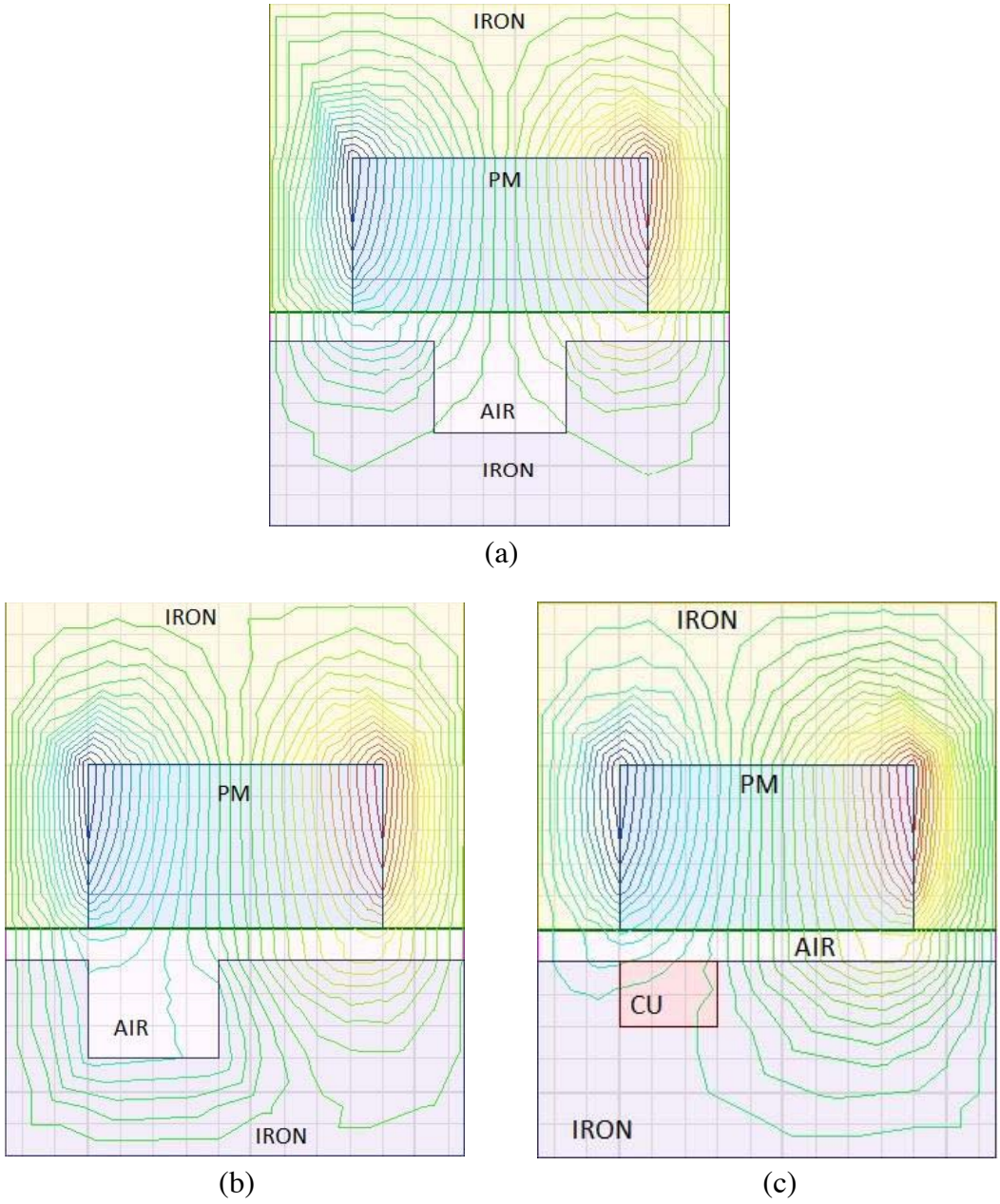

Figure 2. Flux lines in 3 models: (a) symmetrical, (b) asymmetrical and (c) symmetrical with copper.

It is clear that in the above-mentioned modeling, there are no even (for vertical component) and odd (for horizontal component) symmetries of the magnetic field in the PM any more. Therefore, the extracted eigen-functions from the VST, presented in Eq. (16), cannot predict precise behavior of the magnetic field under asymmetrical conditions well, and modification of Eigen function and magnetic potential vector is necessary. Therefore, it is again referred to the system of Equation (12), and by neglecting the magnetic field preassumption symmetry or asymmetry in the PM region, two eigenvalues are determined instead of one eigenvalue, as such that both the equations with non-zero coefficients are held. In this case, we have:

$$\begin{matrix} a_n \neq 0 \\ b_n \neq 0 \end{matrix} \tag{18}$$

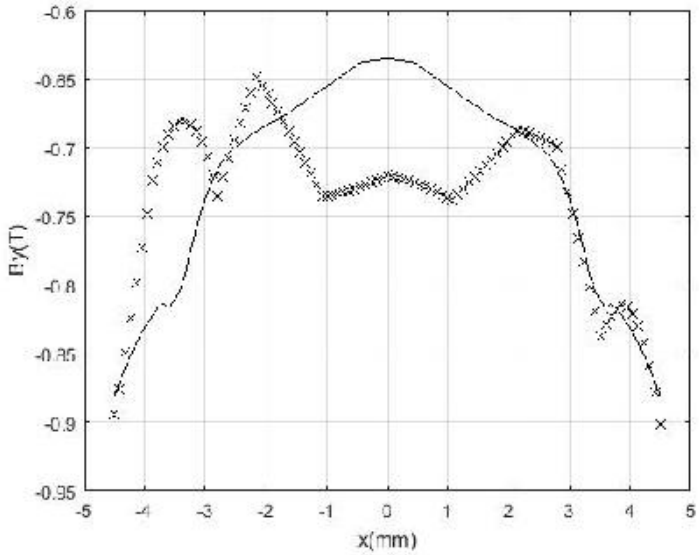

Figure 3. Magnetic flux density of vertical component in PM region (− − −: symmetrical case, x: asymmetrical case).

$$k_{1m} = \frac{(2m-1)\pi}{w}, \quad m = 1, 2, 3, ... \tag{19}$$

$$f_{1m}(x) = \sin\left(\frac{(2m-1)\pi}{w}x\right) \tag{20}$$

$$k_{2n} = \frac{(2n)\pi}{w}, \quad n = 1, 2, 3, ... \tag{21}$$

$$f_{2m}(x) = \cos\left(\frac{(2m)\pi}{w}x\right) \tag{22}$$

$$\begin{aligned} A_{pm}(x,y) = {} & \mu_0 Mx + k_1 + \sum_m a_m \cosh\left[\frac{(2m-1)\pi}{w}(y-h)\right] \sin\left(\frac{(2m-1)\pi}{w}x\right) \\ & + \sum_n b_n \cosh\left[\frac{(2n)\pi}{w}(y-h)\right] \cos\left(\frac{(2n)\pi}{w}x\right) \end{aligned} \tag{23}$$

The elements of Eq. (23) are as such that the magnetic flux density is not necessarily symmetrical and can be modeled under asymmetrical conditions model in the PM, according to the geometry of the machine. Thus, it is necessary to use both eigenvalues for extracting magnetic potential equations.

3. COPPER REGION

Assume that the Cu region is defined as shown in Figure 4. The governing equations in this region are as follows [21]:

$$\overrightarrow{J} = J_0 \hat{k} \tag{24}$$

$$\frac{\partial^2 A_{cu}}{\partial^2 x} + \frac{\partial^2 A_{cu}}{\partial^2 y} = -\mu_0 J_0 \tag{25}$$

Contrary to the governing equations of the PM, the Cu region equation has homogenous boundary conditions, but the equation itself is non-homogenous (Poisson equation).

Considering the geometrical symmetry, it is expected that the horizontal component of the magnetic flux density around the vertical axis has even symmetry, and magnetic flux density vertical component has odd symmetry, which are in fact dual states of the fields relative to the PM region. Therefore,

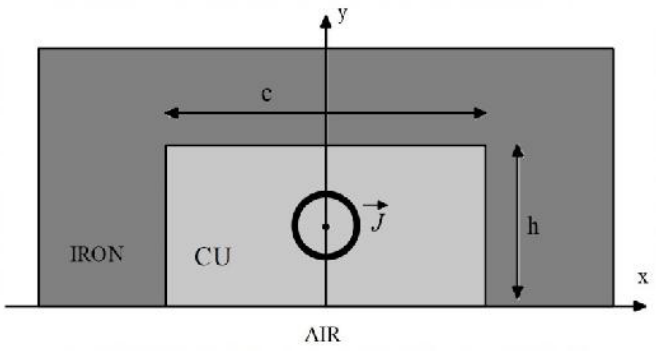

Figure 4. Copper region.

if field equations are extracted based on the even symmetry in the horizontal component, eigenvalue, eigen-function and magnetic potential are extracted as follows:

$$k_n = \frac{(2n)\pi}{c}, \quad n = 1, 2, 3, ... \tag{26}$$

$$f_n(x) = \cos\left(\frac{(2n)\pi}{c}x\right) \tag{27}$$

$$A_{cu}(x, y) = -\frac{1}{2}\mu_0 J_0 y^2 + \mu_0 J_0 h y + k_2 + \sum_n a_n \cosh\left[\frac{(2n)\pi}{c}(y - h)\right]\cos\left(\frac{(2n)\pi}{c}x\right) \tag{28}$$

In Eq. (28), the first three terms are the responses of the non-homogenous equation, and the last term is the response of the homogenous equation. Similar to PM case, it is expected that the magnetic field of the Cu region under asymmetrical conditions around this region is asymmetrical, and therefore, the above equation cannot model the behavior of the actual magnetic field. The eigenvalues and related functions can be fully extracted based on this, and the first eigenvalue and eigen-function, the second (complement) eigenvalue and eigen-function, and the complete form of the equations are determined as follows:

$$k_{1n} = \frac{(2n)\pi}{c}, \quad n = 1, 2, 3, ... \tag{29}$$

$$f_{1n}(x) = \cos\left(\frac{(2n)\pi}{c}x\right) \tag{30}$$

$$k_{2m} = \frac{(2m-1)\pi}{c}, \quad m = 1, 2, 3, ... \tag{31}$$

$$f_{2m}(x) = \sin\left(\frac{(2m-1)\pi}{c}x\right) \tag{32}$$

$$\begin{aligned} A_{cu}(x, y) = {} & -\frac{1}{2}\mu_0 J_0 y^2 + \mu_0 J_0 h y + k_2 + \sum_m a_m \cosh\left[\frac{(2m-1)\pi}{c}(y - h)\right]\sin\left(\frac{(2m-1)\pi}{c}x\right) \\ & + \sum_n b_n \cosh\left[\frac{(2n)\pi}{c}(y - h)\right]\cos\left(\frac{(2n)\pi}{c}x\right) \end{aligned} \tag{33}$$

4. FIELD EQUATIONS FOR TWO ADJACENT PM AND CU REGIONS WITH SYMMETRY

Vernier machine operates based on magnetic flux modulation, in which the PM and Cu regions are placed side-by-side. In such a case, it is necessary to develop the field equations based on the particular conditions caused by the adjacent PM and copper, which leads to different distributions of the magnetic field in these regions. Therefore, attempt is made to develop the governing equations based on sub-

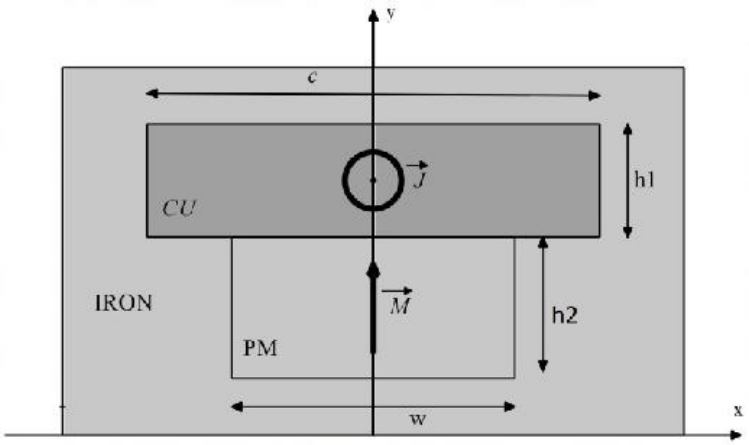

Figure 5. Regions adjacent to PM and symmetrical Cu (around ideal iron).

domain analysis. Figure 5 presents the proposed geometry in which the current in the Cu region is perpendicular to the plane, and the PM momentum is in the vertical axis direction.

Based on the description in Section 3, the field equation in the copper region is as follows:

$$A_{cu}(x,y) = -\frac{1}{2}\mu_0 J_0 y^2 + \mu_0 J_0 h y + k_1 + \sum_m a_{1m}\cosh[m'(y-h)]\sin(m'x) + \sum_n b_{1n}\cosh[n'(y-h)]\cos(n'x) \tag{34}$$

For simplification, the following equivalent expression is used:

$$\begin{aligned} m' &= \frac{(2m-1)\pi}{c}, \quad m = 1,2,3,... \\ n' &= \frac{(2n)\pi}{c}, \quad n = 1,2,3,... \end{aligned} \tag{35}$$

$$h = h_1 + h_2 \tag{36}$$

In addition, equations for the PM region are as follows:

$$A_{pm}(x,y) = \mu_0 J x + k_2 + \sum_p a_{2p}\cosh[p'y]\sin(p'x) + \sum_q b_{2q}\cosh[q'y]\cos(q'x) \tag{37}$$

where:

$$\begin{aligned} p' &= \frac{(2p-1)\pi}{w}, \quad p = 1,2,3,... \\ q' &= \frac{(2q)\pi}{w}, \quad q = 1,2,3,... \end{aligned} \tag{38}$$

To estimate the magnetic field, it is necessary to determine all homogenous equations coefficients of two regions and constant coefficients. Since there are merely two regions in the above-mentioned geometry and the magnetic potential is a relative quantity, for simplification, one of the coefficients such as k_1 is assumed to be zero without any disruption in the results. As seen, the above-mentioned equations over three adjacent regions (ideal core) which care about the boundary conditions, and only remaining boundary of the equations is the boundary between two PM and Cu regions. In this region, continuity of the magnetic potential and tangential component of the magnetic field intensity are held. Therefore:

$$\begin{cases} y = h_2 \\ x \in \left[-\dfrac{w}{2}, +\dfrac{w}{2}\right] \end{cases} \Rightarrow A_{pm}(x,h_2) = A_{cu}(x,h_2) \tag{39}$$

$$\begin{cases} y = h_2 \\ x \in \left[-\dfrac{c}{2}, +\dfrac{c}{2}\right] \end{cases} \Rightarrow H_{xcu}(x,h_2) = \begin{cases} H_{xpm}(x,h_2) \Leftrightarrow x \in \left[-\dfrac{w}{2}, +\dfrac{w}{2}\right] \\ 0 \Leftrightarrow \text{Otherwise} \end{cases} \tag{40}$$

Particularly, the magnetic field intensity equations of 2 regions in the common boundary based on Eqs. (34) and (37) are as follows:

$$H_{xcu}(x,h_2) = -\frac{1}{\mu_0}\left\{\begin{array}{l} -\mu_0 J_0 h_2 + \mu_0 J_0 h \\ +\sum_m m' a_{1m} \sinh[m'(-h_1)]\sin(m'x) \\ +\sum_n n' b_{1n} \sinh[n'(-h_1)]\cos(n'x) \end{array}\right\} \tag{41}$$

$$H_{xpm}(x,h_2) = -\frac{1}{\mu_{pm}}\left\{\begin{array}{l} \sum_p p' a_{2p} \cosh[p'h_2]\sin(p'x) \\ +\sum_q q' b_{2q} \cosh[q'h_2]\cos(q'x) \end{array}\right\} \tag{42}$$

A close look at the magnetic field intensity shows that the Cu region in the boundary has a constant tangential component while this component in the PM region is equal to zero. In other words, considering the magnetic field distribution in the Cu region and turning of the flux lines around this region, it is expected that a part of the tangential field also penetrates inside the PM, while in the obtained equation for the tangential magnetic field intensity in the PM, such a component is absent. Therefore, to care about the boundary conditions, it is necessary to apply some modifications to the magnetic field potential of the PM region. At this end, the following terms are added to the PM magnetic potential:

$$F_{2\mathrm{mod}}(y) = f_1 y^2 + f_2 y \tag{43}$$

where $F_{2\mathrm{mod}}(y)$ is the modification function. Meanwhile, at $y = 0$, the tangential component of the magnetic field intensity is zero, therefore:

$$f_2 = 0 \tag{44}$$

On the other hand, by adding Eq. (42) to Eq. (36), Eq. (1) will be violated. To avoid this, function $-f_1 x^2$ is added to the modified expression. Finally, we have:

$$F'_{2\mathrm{mod}}(y) = f_1 y^2 - f_1 x^2 \tag{45}$$

So, the magnetic potential equation of the PM region is as follows:

$$A_{pm}(x,y) = f_1 y^2 - f_1 x^2 + \mu_0 J x + k_2 + \sum_p a_{2p}\cosh(p'y)\sin(p'x) + \sum_q b_{2q}\cosh(q'y)\cos(q'x) \tag{46}$$

Considering the variations range of $[-w/2, +w/2]$ for the PM region and nature of the expressions $\mu_0 J x$ and $-f_1 x^2$, the Fourier series of the two expressions is as follows:

$$E(p) = \mu_0 J x = \frac{4\mu_0 J}{w}\frac{(-1)^{(p+1)}}{p'} \tag{47}$$

$$F(q) = -x^2 = 4\frac{(-1)^{(q+1)}}{q'} \tag{48}$$

Finally, the magnetic potential equation is modified as follows:

$$A_{pm}(x,y) = f_1 y^2 + \sum_p [E(p) + a_{2p}\cosh(p'y)]\sin(p'x) + \sum_q [f_1 F(q) + b_{2q}\cosh(q'y)]\cos(q'x) \tag{49}$$

Now, by applying the boundary conditions of Eq. (39), we have:

$$f_1 h_2^2 = \frac{1}{w}\int_{-\frac{w}{2}}^{\frac{w}{2}}\left\{\begin{array}{l} -\frac{1}{2}\mu_0 J_0 h_2^2 + \mu_0 J_0 h h_2 + k_1 \\ +\sum_m a_{1m}\cosh[m'(-h_1)]\sin(m'x) \\ +\sum_n b_{1n}\cosh[n'(-h)]\cos(n'x) \end{array}\right\} dx \tag{50}$$

$$E(p)+a_{2p}\cosh(p'h_2) = \frac{2}{w}\int_{-\frac{w}{2}}^{\frac{w}{2}} \left\{ \begin{array}{l} -\frac{1}{2}\mu_0 J_0 h_2^2+\mu_0 J_0 h h_2+k_1 \\ +\sum_m a_{1m}\cosh[m'(-h_1)]\sin(m'x) \\ +\sum_n b_{1n}\cosh[n'(-h)]\cos(n'x) \end{array} \right\} \sin(p'x)dx \tag{51}$$

$$f_1F(q)+b_{2q}\cosh(q'h_2) = \frac{2}{w}\int_{-\frac{w}{2}}^{\frac{w}{2}} \left\{ \begin{array}{l} -\frac{1}{2}\mu_0 J_0 h_2^2+\mu_0 J_0 h h_2 \\ +k_1+\sum_m a_{1m}\cosh[m'(-h_1)]\sin(m'x) \\ +\sum_n b_{1n}\cosh[n'(-h)]\cos(n'x) \end{array} \right\} \cos(q'x)dx \tag{52}$$

In addition, by applying the boundary conditions of Eq. (40), we have:

$$-\mu_0 J_0 h_2+\mu_0 J_0 h = \frac{1}{c}\int_{-\frac{w}{2}}^{\frac{w}{2}} \left\{ \begin{array}{l} 2f_1h_2+\sum_p [p'a_{2p}\sinh(p'h_2)]\sin(p'x) \\ +\sum_q [q'b_{2q}\sinh(q'h_2)]\cos(q'x) \end{array} \right\} dx \tag{53}$$

$$m'a_{1m}\sinh[m'(-h_1)] = \frac{2}{c}\int_{-\frac{w}{2}}^{\frac{w}{2}} \left\{ \begin{array}{l} 2f_1h_2+\sum_p [p'a_{2p}\sinh(p'h_2)]\sin(p'x) \\ +\sum_q [q'b_{2q}\sinh(q'h_2)]\cos(q'x) \end{array} \right\} \sin(m'x)dx \tag{54}$$

$$n'b_{1n}\sinh[n'(-h_1)] = \frac{2}{c}\int_{-\frac{w}{2}}^{\frac{w}{2}} \left\{ \begin{array}{l} 2f_1h_2+\sum_p [p'a_{2p}\sinh(p'h_2)]\sin(p'x) \\ +\sum_q [q'b_{2q}\sinh(q'h_2)]\cos(q'x) \end{array} \right\} \cos(n'x)dx \tag{55}$$

By mathematical manipulation and forming system of equations from the above equations, the unknown coefficients are determined, and then the magnetic field amplitude of each point of the Cu region or PM region is obtained. To confirm the magnetic field potential equations and the coefficients

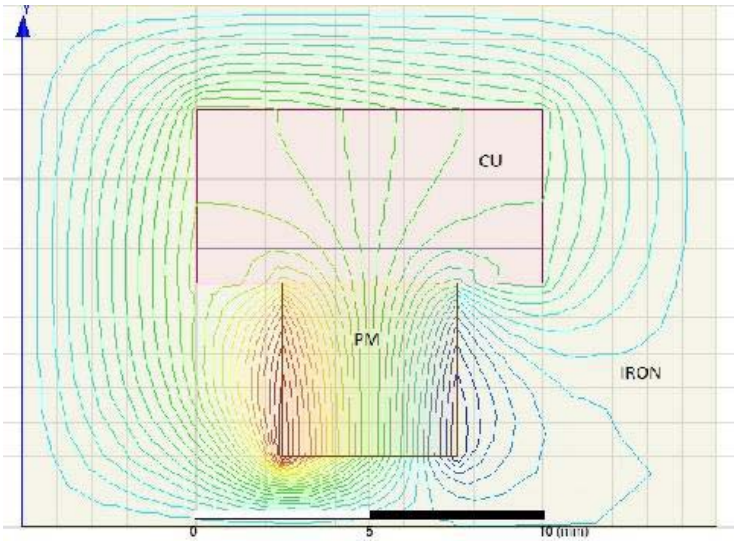

Figure 6. Magnetic field distribution in adjacent regions of PM and symmetrical Cu (around ideal iron).

obtained from solving the above-mentioned system of equations, a geometry according to Figure 6 and specifications of Table 1 is modeled by FEM and compared with the obtained results.

In the first step, to show the accuracy of choosing the eigen-functions and modification terms, amplitude of the tangential components of the field intensity and the vertical magnetic flux density in the boundary of two regions of Figure 7 have been shown. As seen, it cares well the continuity of the

Table 1. Geometrical and materials specifications of model.

Cu region height (mm)	5	PM region height (mm)	5
Cu region width (mm)	10	PM region width (mm)	5
Cu current density (A/m^2)	100000	PM residual magnetic flux density	1.38

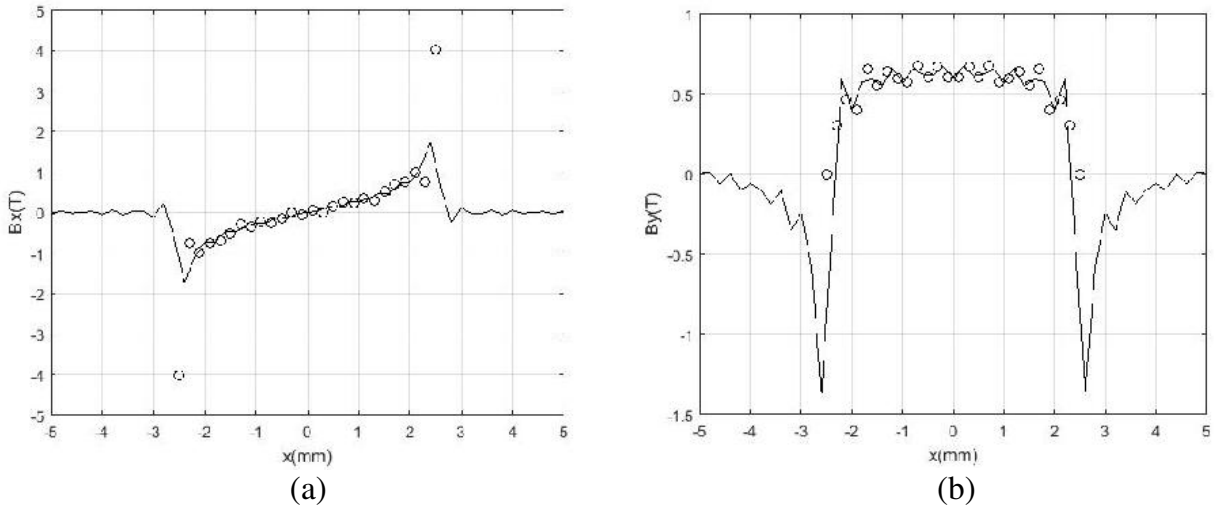

Figure 7. (a) Tangential and (b) vertical components of PM and Cu magnetic flux density on common boundary (ooo PM and −− copper).

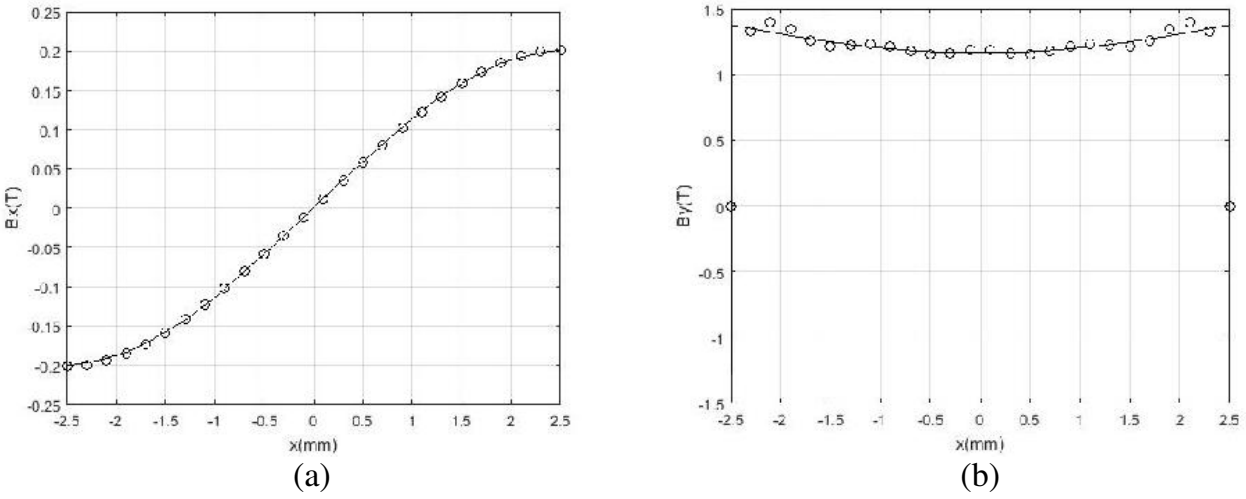

Figure 8. (a) Horizontal and (b) vertical components of PM magnetic flux density on hypothetical line in middle part of PM (ooo SD and −− FE).

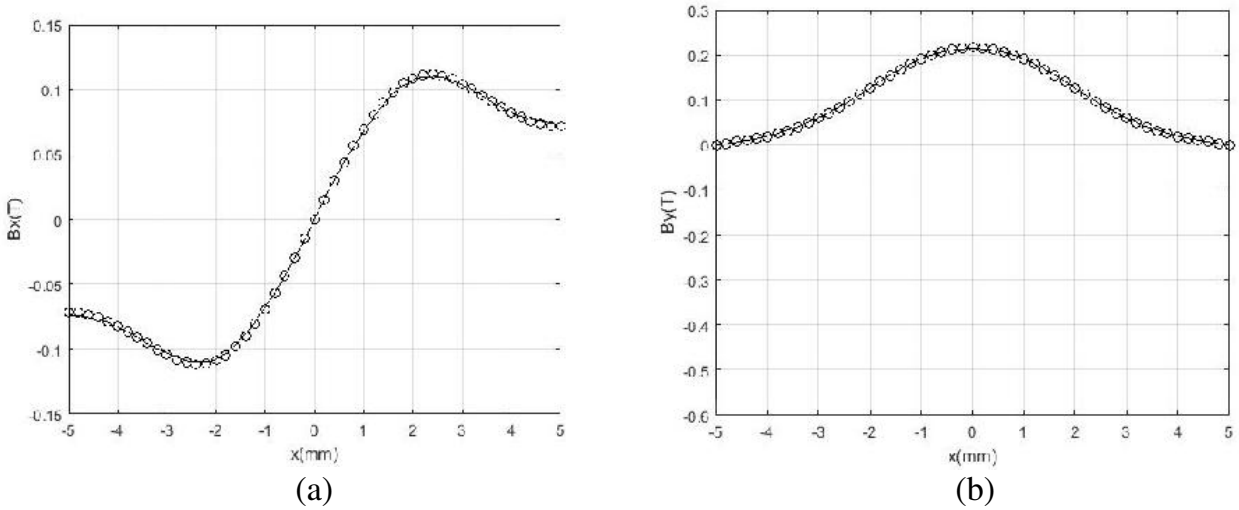

Figure 9. (a) Horizontal and (b) vertical magnetic field on hypothetical line in middle part of Cu (ooo SD and −− FE).

vertical and tangential components of the magnetic field.

In addition, Figures 8 and 9 compare the vertical and horizontal components of the magnetic field on the central line of PM and Cu regions which have been determined by the equations obtained and compared with the results of FEM.

They show that there is a good agreement between the results obtained by the small regions equations and that of the FEM. On the other hand, in the model of Figure 6, the central line of the PM region coincides with the Cu region; therefore, based on the existing symmetry, it can be expected that the horizontal and vertical components of the magnetic field in these regions have odd and even symmetries, respectively. In addition to the FE analysis lines in Figure 6, this symmetry is observable in Figures 8 and 9. Mathematically, due to the symmetry, the coefficients of complementary eigen-functions coefficients, mentioned in Sections 2 and 3, are zero.

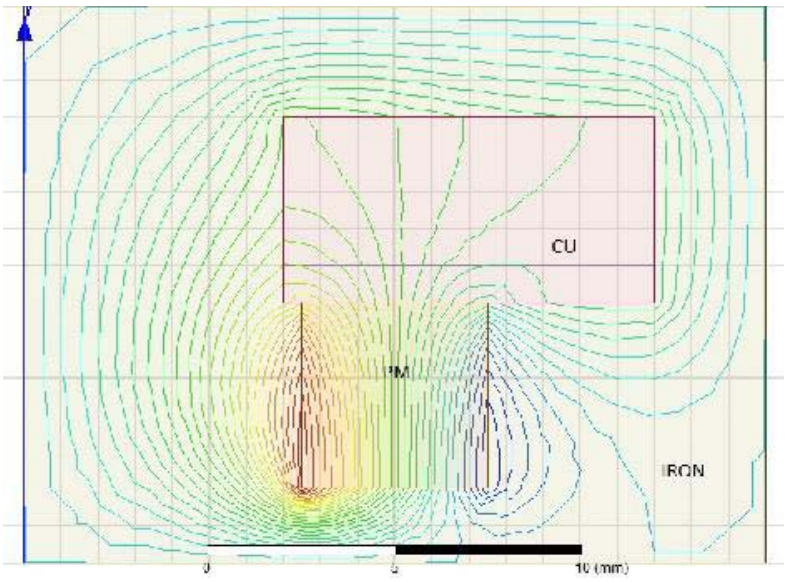

Figure 10. Magnetic field distribution in adjacent regions of asymmetrical PM and copper (around ideal iron).

5. MAGNETIC FIELD EQUATIONS OF TWO ADJACENT PM AND COPPER IN ASYMMETRICAL CASE

To study the impact of the complementary eigen-functions in Sections 2 and 3, the asymmetrical model of Figure 10 is chosen. The magnetic field distribution obtained by FE analysis, particularly in the Cu region, is the result of asymmetry of field. Section 4 presents the procedure for the mathematical analysis. The difference is that considering displacement of the Cu region in the horizontal axis, the magnetic potential of the Cu region is as follows:

$$A_{cu}(x,y) = -\frac{1}{2}\mu_0 J_0 y^2 + \mu_0 J_0 h y + k_1 + \sum_m a_m \cosh[m'(y-h)]\sin(m'(x-x_0)) + \sum_n b_n \cosh[n'(y-h)]\cos(n'(x-x_0)) \quad (56)$$

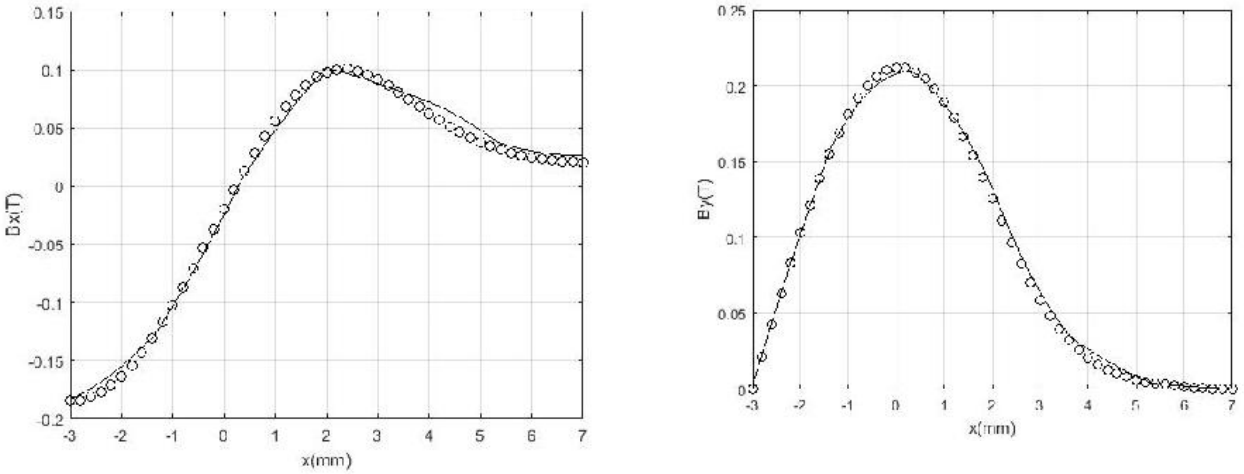

(a) (b)

Figure 11. (a) Horizontal and (b) vertical magnetic flux density on hypothetical line in middle part of Cu in asymmetrical case (ooo SD and −− FE).

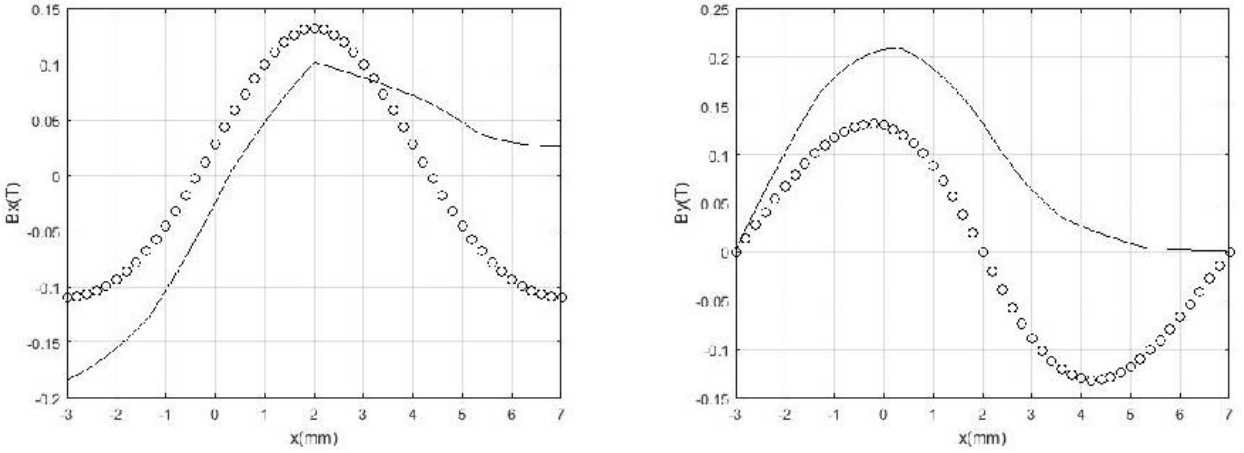

(a) (b)

Figure 12. (a) Horizontal and (b) vertical magnetic flux density on hypothetical line in middle part of Cu in asymmetrical case (ooo Eigenvalue. —– Eigenfunction).

where x_0 is equivalent of Cu displacement on the horizontal axis direction. By applying the boundary conditions on the boundary of two regions, the unknown coefficients of the regions field equations are determined. Figure 11 presents the horizontal and vertical components of the magnetic field in the Cu region.

Meanwhile, the FE analysis is also included in Figure 11. As predicted, symmetries of horizontal and vertical components of the magnetic field have been totally eliminated due to the asymmetry of the model and concentration of the field horizontal component toward the right side and vertical component toward the left side. It is noted that if the complementary eigenvalues and eigen-functions are not used, it is not possible to extract asymmetrical diagrams similar to Figure 11, and consequently, the estimated error of the field rises. For more examination, Figure 12 shows the results of asymmetry model in Figure 10 with merely one eigenvalue and eigen-function. As seen, a major error is accrued in the determination of magnetic fields, such that it cannot be possible to use the obtained magnetic flux density for analyzing magnetic field behavior.

6. CONCLUSION

Choosing eigenvalues and eigen-functions of the Fourier series in the variables separation method is essential for solving the Maxwell equations (Laplacian and Poisson). Generally, a symmetrical magnetic field in the PM or Cu regions merely uses an eigenvalue and eigen-function for these regions. If the geometry is completely or approximately symmetrical, there is not a significant error, but if the asymmetrical geometry exists, estimation of more precise values in the field of the PM or Cu regions is essential. It is necessary to choose complementary eigenvalues and eigen-functions. This paper presents the complementary eigenvalues and eigen-functions in the PM and Cu regions and their effects on the accuracy of SDA for determination of the flux density in PM or Cu domains. Based on the obtained results, considering merely one eigenvalue and eigen-function may generate major errors in flux density up to 50%, or non-valid data depend on asymmetry level. The magnetic field equations in two symmetrical and asymmetrical cases were solved, and the impact of using the complementary eigenvalues and Eigen functions for these regions was addressed. Finally, the results were compared with that of the FE.

REFERENCES

1. Devillers, E., et al., "A review of subdomain modeling techniques in electrical machines: Performances and applications," *XXII International Conference on Electrical on Electrical Machines (ICEM)*, Lausanne, Switzerland, Sep. 4–7, 2016.
2. Roubache, L., K. Boughrara, F. Dubas, and R. Ibtiouen, "Semi-analytical modeling of Spoke-type permanent-magnet machines considering the iron core relative permeability: Subdomain technique and Taylor polynomial," *Progress In Electromagnetics Research B*, Vol. 77, 85–101, 2017.
3. Dubas, F. and K. Boughrara, "New scientific contribution on the 2D subdomain technique in Cartesian coordinates: Taking into account of iron parts," *Math. Comput. Appl.*, 2017.
4. Ivrii, V., *Partial Differential Equations*, Textbook, University of Torento, 2017.
5. Li, J., K. T. Chau, and W. Li, "Harmonic analysis and comparison of permanent magnet vernier and magnetic-geared machines," *IEEE Trans. on Magnetics*, Vol. 47, No. 10, 3649–3652, 2011.
6. Jabbari, A., "Exact analytical modeling of magnetic vector potential in surface inset permanent magnet DC machines considering magnet segmentation," *Journal of Electrical Engineering*, Vol. 69, No. 1, 39–45, 2018.
7. Lubin, T., S. Mezani, and A. Rezzoug, "Two-dimensional analytical calculation of magnetic field and electromagnetic torque for surface-inset permanent-magnet motors," *IEEE Trans. on Magnetics*, Vol. 48, No. 6, 2080–2091, 2012.
8. Jabbari, A., "Analytical modeling of magnetic field distribution in inner rotor brushless magnet segmented surface inset permanent magnet machines," *Iranian Journal of Electrical and Electronic Engineering*, Vol. 14, No. 3, 259–269, 2018.

9. Thierry, L., S. Mezani, and A. Rezzoug, "2D exact analytical model for surface-mounted permanent-magnet motors with semi-closed slots," *IEEE Trans. on Magnetics*, Vol. 47, No. 2, 479–492, 2011.
10. Ma, F., et al., "Analytical calculation of armature reaction field of the interior permanent magnet motor," *Journal of Energies*, Vol. 11, No. 9, 1–12, 2018.
11. Jabbari, A. and F. Dubas, "A new subdomain method for performances computation in interior permanent-magnet (IPM) machines," *Iranian Journal of Electrical and Electronic Engineering*, Vol. 16, No. 1, 26–38, 2020.
12. Hannon, B., P. Sergeant, and L. Dupré, "2-D analytical subdomain model of a slotted PMSM with shielding cylinder," *IEEE Trans. on Magnetics*, Vol. 50, No. 7, 2014.
13. Rahideh, A., H. Moghbelli, and T. Korakianitis, "Two-dimensional analytical magnetic field calculations for doubly-salient machines," *IJST Trans. of Electrical Engineering*, Vol. 38, No. E1, 33–57, 2014.
14. Ben Yahia, M., K. Boughrara, and F. Dubas, "Two-dimensional exact subdomain technique of switched reluctance machines with sinusoidal current excitation," *Math. Comput. Appl.*, Vol. 23, No. 4, 59, 2018.
15. Djelloul-Khedda, Z. and K. Boughrara, "Nonlinear analytical prediction of magnetic field and electromagnetic performances in switched reluctance machines," *IEEE Trans. on Magnetics*, Vol. 53, No. 7, 2017.
16. Oner, Y., et al., "Analytical on-load sub-domain field model of permanent magnet Vernier machines," *IEEE Trans. on Industrial Electronics*, Vol. 63, No. 7, 4105–4117, 2016.
17. Boughrara, K., T. Lubin, and R. Ibtiouen, "General subdomain model for predicting lagnetic field in internal and external rotor multiphase flux-switching machines topologies," *IEEE Trans. on Magnetics*, Vol. 49, No. 10, 5310–5325, 2013.
18. Malé, G., et al., "Analytical calculation of the flux density distribution in a superconducting reluctance machine with HTS bulks rotor," *Elsevier, Mathematics and Computers in Simulation*, Vol. 90, 230–243, 2013.
19. Wu, J., B. Wen, Y. Zhang, and Q. Zhang, "Complete subdomain model for radial-flux slotted PM machines with toroidal windings accounting for the iron-part," *IOP Conference Series: Materials Science and Engineering*, Vol. 569, No. 3, 032054, 2019.
20. Cheng, D. K., *Field and Wave Electromagnetics*, Tsinghua University Press, 2006.